DAVAO RESEARCH JOURNAL
https://davaoresearchjournal.ph

ORIGINAL RESEARCH ARTICLE

Parametric Evaluation and Material Characterization of Garlic Peel-Derived Polyphenol Encapsulation in Water-Soluble Chitosan-Tripolyphosphate Matrices

Lorenz Matthew T. Uy Tan[1], Niccolo Josef T. Gonzales[1], Ben Hur Avian D. Rañeses III[1], Jacen Jerard T. Sy[1], Cynthia F. Madrazo[2], John Ray C. Estrellado [1,2,3] *

[1]Department of Science, Technology, Engineering, and Mathematics, The Academy, De La Salle University, 2401 Taft Ave., Malate, Manila, 1004, Philippines, ORCID No.: Lorenz Matthew T. Uy Tan: https://orcid.org/0009-0002-4137-1548; Niccolo Josef T. Gonzales: https://orcid.org/0009-0000-2466-9014; Ben Hur Avian D. Rañeses III: https://orcid.org/0009-0009-3278-7198; Jacen Jerard T. Sy: https://orcid.org/0009-0007-8534-3369; John Ray C. Estrellado: https://orcid.org/0000-0002-5789-1380
[2]Department of Chemical Engineering, Gokongwei College of Engineering, De La Salle University, 2401 Taft Ave., Malate, Manila, 1004, Philippines, ORCID No.: Cynthia F. Madrazo: https://orcid.org/0000-0003-2531-2353; John Ray C. Estrellado: https://orcid.org/0000-0002-5789-1380
[3]Center for Engineering and Sustainable Development Research, De La Salle University, 2401 Taft Ave., Malate, Manila, 1004, Philippines, ORCID No.: John Ray C. Estrellado: https://orcid.org/0000-0002-5789-1380

*Corresponding author: *john.ray.estrellado@dlsu.edu.ph*

ABSTRACT

Garlic peels remain an underutilized lignocellulosic biomass within the agro-industrial value chain despite their inherent bioactive polyphenol content. However, the thermal and oxidative instability of polyphenols limits high-value valorization of garlic peel biomass and requires stabilization strategies such as encapsulation. This study investigates how water-soluble chitosan (CS) and sodium tripolyphosphate (NaTPP) concentrations affect the encapsulation efficiency of garlic peel polyphenols (GPP) in water-soluble chitosan-tripolyphosphate (CS-TPP) matrices through ionotropic gelation. The highest encapsulation efficiency (EE) observed was 53.02 ± 10.92% with 7% w/v CS and 1% w/v NaTPP. Reduced model ANOVA revealed moderate goodness of fit (R^2 = 0.70; p < 0.0001) and a non-significant lack-of-fit (p = 0.46), with CS concentration (p < 0.0001), NaTPP concentration (p = 0.0130), and NaTPP concentration * NaTPP concentration (p = 0.0015) having significant effects on the encapsulation efficiency. Particle size analysis of GPP encapsulated in CS-TPP (GPP@CS-TPP) and CS-TPP matrices revealed an average particle size of 2.71 mm and 2.55 mm, respectively. Fourier-Transform infrared spectroscopy confirmed the presence of polyphenols in the matrices and the electrostatic interactions between the amide and phosphate groups of CS and TPP. Scanning electron microscopy revealed low crosslinking density at the center of both CS-TPP and GPP@CS-TPP matrices. These findings demonstrate the feasibility of CS-TPP encapsulation in agricultural-waste-derived crude polyphenol extracts and provide insights into concentration-dependent encapsulation performance.

Keywords: *Chitosan, encapsulation, garlic peel, polyphenol, sodium tripolyphosphate*

Submitted: 14 Jun 2026
Revised: 07 Oct 2026
Accepted: 18 Oct 2026
Published: 02 Dec 2026

OPEN ACCESS

How to cite: Uy Tan, L. M. T., Gonzales, N. J. T., Rañeses III, B. H. A. D., Sy, J. J. T., Madrazo, C. F., and Estrellado, J. R. C. (2026). Parametric Evaluation and Material Characterization of Garlic Peel-Derived Polyphenol Encapsulation in Water-Soluble Chitosan-Tripolyphosphate Matrices. *Davao Research Journal*, 17(4), 6-19. https://doi.org/10.59120/drj.v17i4.636

INTRODUCTION

Global garlic production in 2025 was estimated at 30.1 million tons, with China, India, and Bangladesh as the top producers (Adelpour et al., 2025). The garlic processing industry produces approximately 3.7 million tons of waste annually (Azmat et al., 2023). Garlic processing and consumption produce by-products that are often ignored for their potential, such as skins, outer leaves, tops, and bottoms, which raises environmental concerns. In 2022, the Ilocos Region spearheaded the Philippines' garlic production, contributing over 76% of the country's 5,884 metric tons (De Guzman, 2023). However, demand in the Philippines remains too high for local production; for example, the Philippines produced 11,750 metric tons, which was far below the annual demand of 128,000. As a result, the Philippines' import dependence can render local garlic moot due to competition (Cruz, 2021). Addressing the issue requires new perspectives that can utilize the by-products' value in different applications (Adelpour et al., 2025).

Garlic peels, often discarded as agricultural biowaste, can be valorized as an excellent source of polyphenols and other phytochemicals with antimicrobial and antioxidant properties similar to those found in the bulb, with applications in culinary, medicinal, and agricultural uses (Azmat et al., 2023). Previous studies have shown that integrating garlic peel-derived ingredients can enhance the nutritional and functional properties of food products. Garlic peel powder was incorporated as a fortificant in "pukhlein", a traditional rice-based snack, while black garlic powder was investigated in bread formulations to improve functional and sensory properties (Lyngdoh and Ray, 2022; Maietti et al., 2025). In addition, garlic peel extracts have also been utilized as an antimicrobial agent for food packaging applications, effectively eradicating known food spoilage pathogens such as *Staphylococcus aureus, Escherichia coli, Listeria innocua, Salmonella typhimurium*, and *Klebsiella pneumoniae* due to major polyphenol constituents found in the crude extracts of garlic peels (Chaudhary et al., 2021; Hernández-Montesinos et al., 2023). Researchers have also

explored the effects of garlic peel extracts in rat models of ulcerative colitis, where oral administration reduced inflammatory and oxidative stress responses, suggesting their potential as natural antioxidant and anti-inflammatory agents (Althumairy et al., 2025). In the Philippine context, these findings provide a basis for exploring locally sourced garlic peels and garlic peel extracts as value-added ingredients in products such as rice- and wheat-based foods, antimicrobial food packaging, and natural antioxidants. Valorizing garlic peels as a source of polyphenols reduces waste and improves resource utilization under SDG #12: Responsible Consumption and Production, and supports SDG #9: Industry, Innovation, and Infrastructure by developing natural, eco-friendly alternatives to synthetic additives (Azmat et al., 2023).

Although garlic peel extracts have promising applications in the food, health, and packaging industries, polyphenols from plant extracts degrade rapidly under various environmental factors, significantly reducing bioavailability, antimicrobial activity, and shelf life (Thach, 2022). Two conditions strongly affect this instability: surrounding pH and temperature, which play vital roles in regulating degradation (Lee et al., 2014). Temperature and extraction time also strongly affect polyphenol stability, with polyphenols becoming highly unstable at high temperatures and near-neutral pH (Spigno et al., 2007). Processing and storage can also accelerate degradation, limiting extract bioavailability in intended applications (Thach, 2022). Polyphenol extraction also presents stability issues, particularly when large volumes of organic solvents and their toxic residues are used, which can harm human health and are major concerns in food and cosmetic applications (Chhouk et al., 2017). Among common extraction solvents, ethanol is often preferred because it extracts active ingredients better than other solvents and is readily available (Subroto et al., 2021).

Encapsulation is a widely used method to address and improve the instability of phenolic compounds, especially in plants (Bińkowska et al., 2024). Encapsulation involves trapping active agents, such as susceptible plant polyphenols, within a natural protective matrix to create a barrier between the core substance and external chemical and environmental factors, thereby preventing degradation (Barbosa-Nuñez et al., 2025). Natural polymers such as gums, pectin, and gelatin are the most widely used for food encapsulation because of their physicochemical and biological properties. Another natural polymer, chitosan (CS), is a biodegradable, linear polysaccharide usually produced by deacetylation of chitin, a main component of crustacean exoskeletons. CS is commonly chosen for its beneficial properties, including biocompatibility, biodegradability, and low toxicity, enabling applications in food preservation, medicine, and related areas of study (Detsi et al., 2020). Encapsulation can be conducted through multiple methods, such as spray coating, spray drying, and solvent evaporation (Sacco et al., 2016). CS encapsulation is primarily achieved through ionotropic gelation because it is simple and uses mild conditions (Pant and Negi, 2018). In key fields such as biomedicine and food, ionotropic gelation stands out among encapsulation methods for its simplicity, versatility, and use of biodegradable, biocompatible polymers, which support environmental sustainability (Sacco et al., 2021). The technique relies on the interaction between positively charged amino groups in CS and the negatively charged groups of a polyanion, often called a crosslinker. Among crosslinker options, sodium tripolyphosphate (NaTPP) is the most commonly paired crosslinker with CS because of its safety and multivalent properties (Preciado-Rangel et al., 2025).

Encapsulation efficiency (EE), which quantifies the proportion of the initial core material successfully retained within an encapsulation matrix, is a widely measured parameter for evaluating the effectiveness and material efficiency of bioactive encapsulation systems (Yang et al., 2013; Zhang et al., 2010). CS and NaTPP concentrations can substantially affect the physicochemical characteristics of the resulting particles, including particle size, morphology, and stability (Estevinho and López-Rubio, 2024). Multivariate analyses of chitosan-tripolyphosphate (CS-TPP) encapsulation matrices have shown that CS and NaTPP concentrations influence the structural characteristics of the resulting matrix, such as mass and particle size (Giraldo et al., 2019). Thus, exploring the effects of varying these concentrations may help retain bioactive compounds and control particle formation efficiently.

Although CS-TPP systems have been extensively investigated, most of the literature has focused on developing nano-sized particles (Kim et al., 2022; Ma et al., 2022), with few studies focusing on macro-sized particles (Iswandana et al., 2017). In food processing industries, macro-sized particles offer practical advantages, such as easier solids handling, recovery, and incorporation in unit operations and processes, which are inherent limitations of nanoparticles (Assadpour and Jafari, 2019; English et al., 2023). However, limitations in previous studies that used CS concentrations to produce nano-sized or micro-sized CS-TPP particles cannot be extrapolated to the formation of larger matrices, underscoring the need to study the development of macro-sized encapsulation systems with adjusted CS concentrations. In addition, systematic evaluation of the effects of CS and NaTPP concentrations on encapsulation remains limited, particularly in macroscopic CS-TPP matrices (Pistone et al., 2023). Thus, this study provides preliminary insights into the concentration-dependent encapsulation efficiency and physicochemical properties of CS-TPP matrices containing crude garlic peel polyphenols by determining the total phenolic content, total flavonoid content, and DPPH• radical scavenging activity of the GPP ethanolic crude extract, evaluating the effects of CS and NaTPP concentrations on encapsulation efficiency, and characterizing the CS-TPP matrices and the selected GPP-encapsulated matrix in terms of Fourier-transform infrared spectroscopy (FTIR), particle size analysis, and scanning electron microscopy (SEM).

MATERIALS AND METHODS

Materials and chemicals

Garlic peels were acquired from Dizon Farms, Taguig City, Metro Manila, Philippines. Folin-Ciocalteu (FC) reagent was purchased from Los Baños, Laguna, Philippines. Sodium carbonate (Na_2CO_3), quercetin ($C_{15}H_{10}O_7$), 2,2-diphenyl-1-picrylhydrazyl (DPPH), and aluminum chloride (AlCl3) were obtained from DKL Laboratory Supplies, Manila City, Philippines. Gallic acid ($C_7H_6O_5$) was purchased from Loba Chemie (Mumbai, India). Trolox ($C_{14}H_{18}O_4$) was obtained from Phygene Scientific Co., Ltd. (Fuzhou, China). Sodium acetate (CH_3COONa) was purchased from Ajax Finechem (New South Wales, Australia). Water-soluble chitosan (CS) was purchased from Xi'an Qinghekang Co., Shaanxi, China. Sodium tripolyphosphate (TPP) was obtained from Dalkem Corporation, Quezon City, Philippines.

Experimental design

The study used a two-factor, three-level full factorial (3^2) experimental design. CS and TPP concentrations were the two factors used to measure the encapsulation efficiency (EE) of the encapsulated garlic peel polyphenols (GPP). As presented in Table 1, each level was characterized as low (-1), middle (0), and high (+1). The levels of each factor were 1%, 2%, and 3% w/v for NaTPP concentration, and 3%, 5%, and 7% w/v for CS concentration.

Table 1. Factors and coded levels for the preparation of GPP using CS-TPP matrices.

Factors	Low (-1)	Middle (0)	High (+1)
Chitosan Concentration (%w/v), A	3	5	7
Tripolyphosphate Concentration (% w/v), B	1	2	3

*Note: GPP=Garlic Peel Polyphenol; CS=Chitosan; TPP= Tripolyphosphate

The values for each factor were modelled after a second-order polynomial equation, adopted from Palero et al. (2026), as follows:

$$EE=\beta_0+\beta_a A+\beta_b B+\beta_{ab} AB+\beta_{aa} A^2+\beta_{bb} B^2$$

The dependent *EE*, encapsulation efficiency, is expressed as a function of chitosan concentration (A) and TPP concentration (B). In the second-order model, β_0 serves as the intercept; β_a and β_b are the linear coefficients of *A* and *B*, respectively; β_{ab} is the interaction coefficient between *A* and *B*; and β_{aa} and β_{bb} are the quadratic coefficients of *A* and *B*, respectively.

Extraction of garlic peel polyphenols

A portion of the methodology conducted by Hernández-Montesinos (2023) was adopted with modifications to extract the GPP. Garlic peels were disinfected, ground, and passed through a 60-mesh sieve. They were then macerated with a 1:10 solute-to-solvent ratio in 80% (v/v) ethanol. The mixture was filtered to obtain the filtrate, which was then rotary-evaporated at 40 °C to remove the ethanol. The sample was then freeze-dried. Finally, 1 mg/mL GPP was dissolved in 80% (v/v) ethanol solution.

Phytochemical quantification of garlic peel polyphenols

A total of 100 µL of the GPP solution was reacted with 400 µL of FC reagent and 2000 µL of 1 mg/mL Na_2CO_3 and incubated for 2h at room temperature, protected from light, as adopted from Hernández Zarate et al. (2018) with modifications. The mixture's absorbance at 765 nm was then measured using a Dynamica Halo VIS-20 spectrophotometer (Dynamica Pty Ltd, Clayton, Victoria, Australia) to determine the total phenolic content (TPC). Polyphenols were reported as µg gallic acid equivalent (GAE). The calibration curve was created using gallic acid concentrations ranging from 10 to 50 µg/mL.

Total Flavonoid Content (TFC) was determined following the methods of Hernández Zarate et al. (2018), with modifications. Reagents, which include 100 µL of CH_3COONa and 100 µL of $AlCl_3$, were mixed with 100 µL of the GPP solution. The mixture was then diluted with 1700 µL of 80% (v/v) ethanol and left at room temperature for 40 min. Absorbance at 415 nm was then measured and expressed in µg quercetin equivalents (QE). The standard curve was generated using quercetin concentrations from 50 to 250 µg/mL (Hernández Zarate et al., 2018; Hernández-Montesinos et al., 2023).

Radical Scavenging Activity (RSA) was conducted according to Stoica et al. (2013). DPPH• was dissolved in 80% (v/v) ethanol; 2100 µL of the solution was then reacted with 900 µL of 2 mg/mL GPP in distilled water. The mixture was shaken and left in the dark for 30 min. A control solution of 3,000 µL of DPPH• was prepared. The decrease in absorbance was then measured at 517 nm. The antioxidant activity percentage was calculated using the equation below:

$$RSA,\ (\%) = \left(\frac{A_{control}-A_{samp}}{A_{control}}\right)\cdot 100\%$$

where $A_{control}$ and A_{sample} refer to the absorbances of the prepared control and sample, respectively (Stoica et al., 2013).

Encapsulation of garlic peel polyphenols in CS-TPP matrices

The ionotropic gelation method was used to encapsulate GPP in CS-TPP matrices (Stoica et al., 2013). This method works because polyanionic TPP ions stabilize the positively charged amino groups in CS through electrostatic interactions, forming stable matrices via ionotropic gelation. The CS solutions at the concentrations specified in Table 1 were mixed with 50 mL of GPP solution. Subsequently, 4 mL of the resulting mixture was loaded into a syringe fitted with a 20 G needle and dispensed dropwise into 50 mL of NaTPP solution at the specified concentrations. The NaTPP solution was maintained under stirring, and the mixture was delivered using a syringe pump at a flow rate of 5 mL/h. The formed matrices were then left stirring for 30 min before being strained. The filtered matrices were freeze-dried at -50 °C.

Determination of encapsulation efficiency

Encapsulation efficiency (EE) was measured according to Stoica et al. (2013), with modifications. To determine the amount of unencapsulated polyphenols, the TPP solution was kept after straining the formed matrices, and the TPC was measured using the Folin-Ciocalteu (FC) method. TPC encapsulated was also measured by redissolving in 80% (v/v) ethanol, centrifuging the samples at 4000 rpm for 5 min, and measuring the TPC of the supernatant using the FC method. The encapsulation efficiency of each trial was computed using the following formula:

$$EE,\ (\%) = \left(\frac{TPC_{encapsulated}}{TPC_{total}}\right)\cdot 100\%$$

where $TPC_{encapsulated}$ is the mass of the phenolic content measured above, while TPC_{total} is the sum of the encapsulated and unencapsulated TPC.

Fourier-transform infrared spectroscopy

The fourier-transform infrared (FTIR) spectrometer was used in attenuated total reflectance (ATR) mode, following parameters reported in previous studies using a Shimadzu IRSpirit spectrometer (Picar et al., 2025; Vergel De Dios et al., 2025). Randomly collected samples were scanned at a frequency range of 4000–400 cm^{-1} with 32 scans.

Particle size analysis

Fifty random representative samples from the parameter combination with the highest encapsulation efficiency were taken and processed through ImageJ 1.54g Edition software (National Institutes of Health, Bethesda, Maryland, USA) to determine their Feret diameter measurements (Igathinathane et al., 2008).

Scanning electron microscopy

The surface and cross-section of representative blank matrices and matrices yielding the highest EE were observed under a scanning electron microscope (SEM). An electron beam with an accelerating voltage of 15 kV was applied to the samples. SEM micrographs were captured at 300, 1000, 3000, 6000, and 12000x magnification.

Statistical analysis

Experiments were performed using a 3^2 factorial design of experiments with the factors and levels shown in Table 1. Four independent experimental replicates (n = 4) were generated using JMP Student Edition 19 software in randomized order to reduce the possibility of systematic bias from treatment combinations and run sequence, for a total of 36 independent randomized experimental runs. Table 2 summarizes the experimental design and order. The parameters for the model were evaluated and fitted using standard least squares, and tested through statistical diagnostics such as Levene's test for homogeneity of variances and the Shapiro-Wilk test for normality. To evaluate the significance of the linear and quadratic terms, the model responses were analyzed using the analysis of variance (ANOVA) at a 5% significance level ($p < 0.05$). Meanwhile, the goodness of fit for the model was assessed using the corresponding coefficient of determination R^2 and the adjusted R^2. The statistical analyses and fit modelling were all performed through the JMP Student Edition 19 software.

Table 2. Full design of experiment and experimental results for the encapsulation of GPP in CS/TPP matrix.

Run	Pattern*	CS (%)	TPP (%)	EE (%)
1	33	7	3	47.86
2	23	5	3	16.52
3	23	5	3	25.49
4	32	7	2	47.76
5	32	7	2	51.85
6	11	3	1	12.51
7	22	5	2	47.94
8	32	7	2	48.81
9	31	7	1	53.38
10	22	5	2	34.21
11	31	7	1	38.22
12	21	5	1	15.12
13	32	7	2	50.6
14	11	3	1	17.26
15	33	7	3	32.04
16	31	7	1	64.4
17	33	7	3	26.93
18	13	3	3	16.29
19	13	3	3	14.25
20	11	3	1	17.35
21	12	3	2	34.62
22	23	5	3	24.06
23	12	3	2	17.02
24	22	5	2	55.07
25	31	7	1	56.06
26	33	7	3	31.77
27	21	5	1	47.94
28	23	5	3	40.2
29	13	3	3	10.73
30	13	3	3	12.57
31	22	5	2	33.86
32	21	5	1	37.43
33	11	3	1	19.49
34	21	5	1	30.91
35	12	3	2	31.31
36	12	3	2	28.57

*Note: GPP=Garlic Peel Polyphenol; CS=Chitosan; TPP= Tripolyphosphate; EE= Encapsulation Efficiency. Pattern is in terms of coded levels. The first digit refers to the coded levels of the CS concentration (1 – 3%, 2 – 5%, 3 – 7%), while the second digit refers to the coded levels of the NaTPP concentration (1 – 1%, 2 – 2%, 3 – 3%). For example, in run 1, "33" means that the encapsulation experiment was performed at a CS concentration of 7% and a NaTPP concentration of 3%;

RESULTS

Phytochemical quantification of GPP

The TPC was calculated using a gallic acid standard calibration curve (Figure 1). The curve showed high validity and linearity, with a coefficient of determination (R^2) of 0.99, confirming a reliable linear relationship for quantification. Using this curve, the TPC was calculated as 75.45 mg GAE/g.

Similarly, the TFC was calculated using a quercetin standard calibration curve (Figure 2). The curve showed strong statistical validity, with a coefficient of determination (R^2) of 0.99,

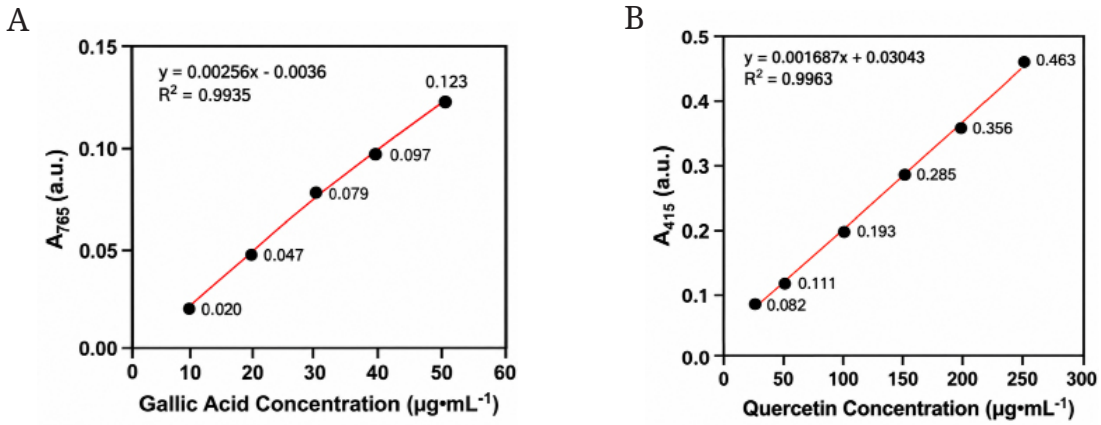


Figure 1. Calibration curve: (A) gallic acid for determination of total phenolic content; (B) quercetin for determination of total flavonoid content.

Encapsulation efficiency of GPP in CS-TPP matrices

Table 3 summarizes the encapsulation efficiency obtained from varying combinations of CS and NaTPP concentrations. The highest EE value (53.02% ± 10.92%) was obtained at 7% CS concentration and 1% NaTPP concentration. The experimental results showed a range of values, with the highest encapsulation efficiency (EE) of 53.02% ± 10.92% and the lowest EE of 13.46% ± 2.37%. When NaTPP concentration was held at 2%, and CS concentrations were tested at different levels, the resulting EE were 27.88% ± 7.65%, 42.77% ± 10.50%, and 49.76% ± 1.82% for NaTPP concentrations of 3%, 5%, and 7%, respectively. This suggests a positive trend in EE in CS-TPP matrices as CS concentration increases in increments. Moreover, when CS concentration was held constant at 5%, the resulting EE were 32.85% ± 13.75%, 42.77% ± 10.50%, and 26.57% ± 9.90% for NaTPP concentrations of 1%, 2%, and 3%, respectively. The trend suggests a non-linear relationship between the determined EE and the NaTPP concentration.

Table 3. Encapsulation efficiency of GPP in CS-TPP matrices under varying CS and TPP concentrations.

CS (%)	NaTPP (%)	EE* (%)
3	1	16.65 ± 2.95
	2	27.88 ± 7.65
	3	13.46 ± 2.37
5	1	32.85 ± 13.75
	2	42.77 ± 10.50
	3	26.57 ± 9.90
7	1	53.02 ± 10.92
	2	49.76 ± 1.82
	3	34.65 ± 9.11

Note: GPP=Garlic Peel Polyphenol; CS=Chitosan; TPP= Tripolyphosphate; EE= Encapsulation efficiency; Encapsulation efficiency was evaluated in four independent experimental replicates (n = 4).

To assess the goodness of fit of the model generated by the factorial experiment, and to test the adequacy of each factor, a one-way ANOVA was performed at a 95% confidence level (α = 0.05). ANOVA results for the full EE model showed a desirable coefficient of determination (R^2) of 0.73, as shown in Table 4. Adjusted R^2 was calculated to be 0.67, which means that the R^2 determined from the model fitting indicates relatively good simulation of the experiment. The root mean square error (RMSE) was 8.45, with a coefficient of variation of 25.55%, indicating substantial spread relative to the mean. The lack-of-fit was also non-significant (p = 0.68), further supporting the full model's suitability for describing EE in terms of the identified factors. Statistically significant terms in the full EE model include CS concentration (A) (p < 0.0001), NaTPP concentration (B) (p = 0.01, and NaTPP concentration * NaTPP concentration (B2) (p = 0.001).

Table 4. Analysis of Variance (ANOVA) of the full encapsulation efficiency (EE) model.

Source	SS	df	MS	*F*-value	*p*-value
Model	5869.74	5	1173.95	16.44	< **0.0001**
A	4205.73	1	4205.73	58.91	< **0.0001**
B	516.48	1	516.48	7.23	**0.01**
AB	230.33	1	230.33	3.23	**0.08**
A^2	17.83	1	17.83	0.25	0.62
B^2	899.38	1	899.38	12.60	**0.001**
Residuals	2141.91	30	71.40		
Corr. Total	8011.65	35			
Lack-of-fit	114.61	3	38.20	0.51	0.68
Pure error	2027.30	27	75.09		
RMSE	8.45		R^2	0.73	
Mean	33.07		Adjusted R^2	0.69	
% CV	25.55		Pred. R^2	0.62	

The removal of non-significant terms through model reduction was performed as described in previous studies to further improve the model's statistical power (Palero et al., 2026). Statistically significant factors, namely CS concentration (A) (p < 0.0001), NaTPP concentration (B) (p = 0.01), and NaTPP concentration * NaTPP concentration (B^2) (p = 0.001) were also found to be statistically significant in the reduced model (Table 5). Although the reduced model R^2 (R^2 = 0.70) was lower than the full model R^2 (R^2 = 0.73), it was closer to the predicted reduced model R^2 (0.63). This suggests that the model has been improved and is less susceptible to overfitting. The lack-of-fit p-value remained non-significant (p = 0.46), indicating that the regression model adequately captures the data trend without systematic errors. The reduced regression equation describing EE in terms of the significant coded factors is shown below.

$$y = 41.13 + 13.24A - 4.64B - 10.60B^2$$

Table 5. Analysis of variance (ANOVA) of the reduced encapsulation efficiency (EE) model.

Source	SS	df	MS	*F*- value	*p*- value
Model	5621.58	3	1873.86	25.09	< **0.0001**
A	4205.73	1	4205.73	56.31	< **0.0001**
B	516.48	1	516.48	6.92	**0.01**
B^2	899.38	1	899.38	12.04	**0.001**
Residuals	2390.07	32	74.69		
Corr. Total	8011.65	35			
Lack-of-fit	362.77	5	72.55	0.97	0.46
Pure error	2027.30	27	75.09		
RMSE	8.64		R^2	0.70	
Mean	33.07		Adjusted R^2	0.67	
% CV	26.14		Pred. R^2	0.63	

Levene's test was non-significant (p = 0.13), and the Shapiro-Wilk test for residual normality was also non-significant (p = 0.57). Figure 3 illustrates the different plots for each data point. Figure 3a shows the externally studentized estimates; Figure 3b shows the residuals-by-predicted plot; Figure 3c shows the actual-versus-predicted plot; and Figure 3d shows the normal quantile plot for the ten tested samples with a fitted Gaussian curve. The non-significant p-value of Levene's test indicates that all data points for EE affected by CS and TPP concentrations have equal variances. Residual plots showed no evident patterns or trends over time, supporting the assumption of independence and confirming that there are few to no outliers in the data points.

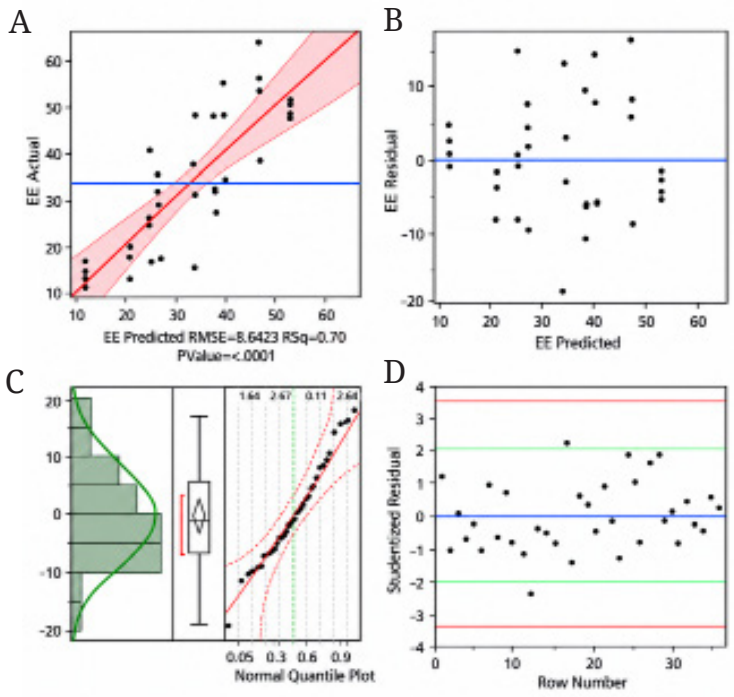


Figure 3. Reduced model diagnostic plots for encapsulation efficiency: (A) predicted vs. actual EE, (B) residual vs. predicted EE, (C) residual normal quantile plot, and (D) studentized residual vs. row number plot.

Pareto chart showing the logworth of the linear and quadratic factors was generated using the JMP Graph Builder interface (Figure 4). A value greater than the logworth at p = 0.05 (Logworth = 1.310) indicates a statistically significant factor. The highest logworth obtained was CS (A) (Logworth = 7.82), followed by NaTPP concentration * NaTPP concentration (B*B) (Logworth = 2.82), and NaTPP concentration (B) (Logworth = 1.89), respectively. Among the significant terms, CS concentration had the greatest influence on the EE of the CS-TPP matrices. CS concentration (A) showed the strongest influence with a positive t-ratio (7.50), whereas factors B and B2 yielded negative t-ratios (-2.63 and -3.47, respectively). The matrices prepared using 7% w/v CS and 1% w/v NaTPP were selected for further material characterization based on their highest experimentally observed mean encapsulation efficiency (53.02% ± 10.92%).

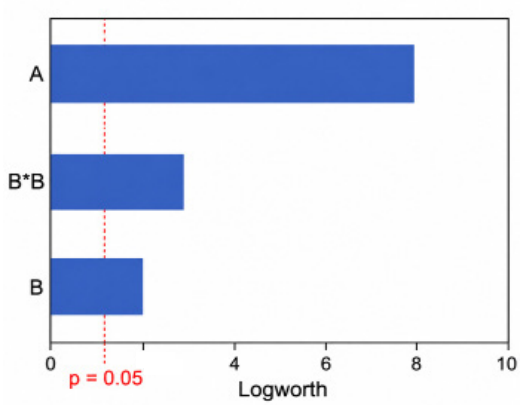


Figure 4. Pareto chart of standardized model parameters showing factor significance.

Fourier-Transform infrared spectroscopy

The FTIR spectra of crushed GPP-encapsulated CS-TPP matrices (GPP@CS–TPP), blank CS-TPP matrices, GPP, and CS were compared (Figure 5). Spectral features were observed across 3,000-3,600 cm^{-1}, 1,550-1,650 cm^{-1}, 1,090 cm^{-1}, and approximately 900 cm^{-1}. The broad band at 3,000-3,600 cm^{-1} was observed in the spectra of CS, GPP, blank CS-TPP, and GPP@CS-TPP. Bands in the 1,550-1,650 cm^{-1} region were apparent in the CS-TPP samples but were not evident in the GPP spectrum. Shifts in the bands were observed when comparing CS with blank CS-TPP and GPP@CS-TPP, particularly in the 1,550–1,650 cm^{-1} and approximately 1,090 cm^{-1} regions. A band near 900 cm^{-1} appeared in the blank CS-TPP and GPP@CS-TPP spectra but was not evident in the CS and GPP spectra. Overall, the GPP@CS-TPP and blank CS-TPP spectra exhibited similar profiles, with some differences in band positions and in the O-H stretching region.

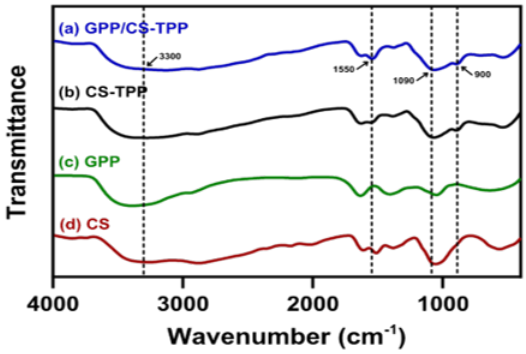


Figure 5. FTIR spectra of (a) garlic peel polyphenol (GPP)-encapsulated water-soluble chitosan-tripolyphosphate matrices (GPP@CS-TPP), (b) CS-TPP matrices, (c) GP, and (d) CS.

Particle size analysis

The particle sizes of the created matrices follow Gaussian distributions, as visualized in Figure 6. The mean particle size of GPP@CS-TPP is 2.71 mm, while CS-TPP matrices have a mean size of 2.55 mm, representing a roughly 0.16 mm (approximately 6.3%) increase in diameter after GPP encapsulation.

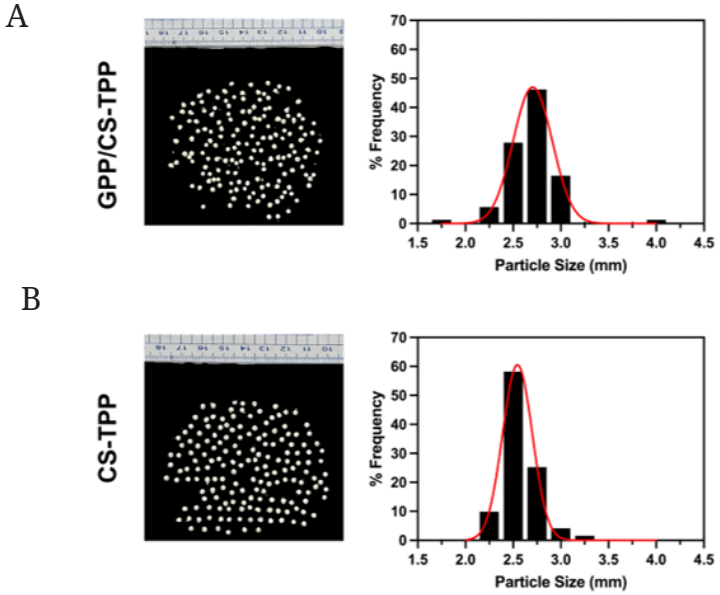


Figure 6. Particle size distribution: (A) garlic peel polyphenol (GPP)-encapsulated chitosan-tripolyphosphate (GPP@CS-TPP), and (B) CS-TPP matrices.

Scanning electron microscopy

The cross-sectional SEM images of both blank CS-TPP and GPP@CS-TPP matrices revealed flaky, hollow internal structures, suggesting heterogeneous morphology across the matrix cross-sections (Figure 7). Both formulations also showed rough, porous surfaces. Despite these morphological features, the GPP@CS-TPP matrices retained overall structural integrity after drying, with no apparent fracturing in the examined images.

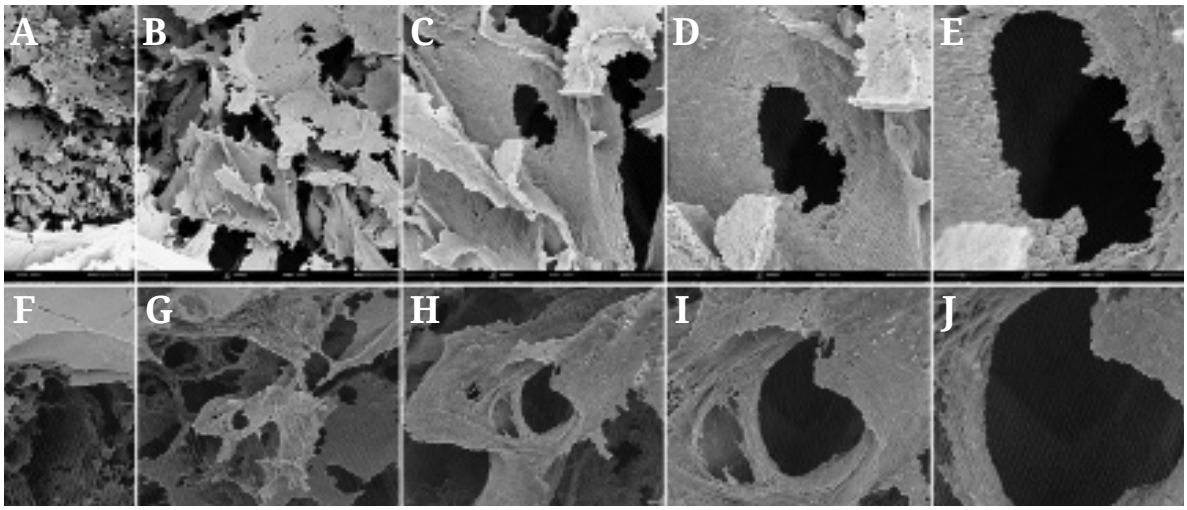


Figure 7. SEM images of water-soluble chitosan-tripolyphosphate (CS-TPP) cross-section in (A) 300x, (B) 1000x, (c) 3000x, (D) 6000x, and (E) 12000x magnification; and garlic peel polyphenol (GPP)-encapsulated CS-TPP matrices (GPP@CS-TPP) cross-section in (F) 300x, (G) 1000x, (H) 3000x, (I) 6000x, and (J) 12000x magnification.

DISCUSSION

Phytochemical quantification of garlic peel polyphenols

The average TPC calculated in this study was significantly lower than the 146.57 mg GAE/g reported in Dos Santos et al. (2022), despite both studies using ethanol as a solvent. However, the ethanolic extract outperformed several studies using aqueous extractions. Specifically, the findings reported by Naqvi et al. (2020) at 51.66 mg GAE/g, Hernández-Montesinos et al. (2023) at 50.41 mg GAE/g, and Santos et al. (2022) at 39.11 mg GAE/g are all less than the average TPC obtained in this work (Hernández-Montesinos et al., 2023; Naqvi et al., 2020). Moreover, the determined TFC was consistent with Fortunata et al. (2019), who observed that ethanol extracts (14.019 mg QE/g) performed better than aqueous extracts (7.59 mg QE/g). Additionally, this value was also higher than the aqueous TFC reported by Naqvi et al. (2020), which reached 7.782 mg QE/g (Fortunata et al., 2019; Naqvi et al., 2020).

The higher yields of both total phenolic content (TPC) and total flavonoid content (TFC) with an ethanolic solvent than with pure water emphasize how solvent-solute dynamics can be critical for recovering polyphenols from garlic peels. The results show ethanol's superior ability to dissolve specific compounds in garlic peels compared with pure water. Extraction efficiency is strongly influenced by the chemical structure and matching solubility parameters of the target solutes within the plant material (Alara et al., 2021). In the case of garlic peel polyphenols (GPP), bioactive compounds in garlic happen to dissolve better in ethanol than in pure water. Furthermore, the consistently higher TFC values validate that flavonoid, which are mostly hydrophobic or semi-polar, dissolve much more efficiently in an alcoholic solvent (Hernández-Montesinos et al., 2023). Variations in parameters such as extraction temperature and duration heavily influence the preservation of the target solute. Because polyphenols contain thermosensitive bonds, prolonged thermal exposure can degrade their antioxidant capacity and structure (Dos Santos et al., 2022; Llarena et al., 2026).

Furthermore, garlic peel phytochemistry varies by genetic background, environmental growth conditions, and cultivar, which explains analytical variation across the literature (Lasalvia et al., 2022). The extraction method also strongly influences polyphenol yield from garlic peel biomass. While this study used maceration, non-thermal methods such as ultrasound-assisted extraction (UAE) and high-pressure assisted extraction (HPAE) can extract higher-quality bioactive compounds because they avoid heat, which can diminish quality (Rathod et al., 2023).

The radical scavenging activity of the crude GPP extract was significantly higher than the values reported by Cocom et al. (2025), where fermented garlic extract in 95% ethanol exhibited an RSA of only 46.3% after one day of extraction at a concentration of 500 µL/mL. These findings establish that the GPP extract has a diverse and abundant phytochemical profile, especially phenolic compounds, depending on the source and pre-processing conditions. Additionally, the high antioxidant activity at low concentrations suggests that GPP compounds are highly effective at neutralizing free radicals (Cocom et al., 2025). Although the polyphenol content was low relative to existing studies, the radical scavenging activity indicates strong antioxidant capacity in the extracted GPP. The highly reactive hydroxyl groups of polyphenols directly react and stabilize unstable free radicals, rendering them inactive (Rathod et al., 2023). Therefore, having a high TPC and TFC in the GPP extract makes it effective in interfering with radical-producing systems, making it an effective natural antioxidant.

Encapsulation efficiency and leakage of CS-TPP systems

The R^2 value obtained for the final reduced model (R^2 = 0.70) indicates a moderate goodness of fit. In contrast, the reduced model's adjusted R^2 (R^2 = 0.67) indicates that some variability remains in the model. However, it is lower than the full model's R^2 and adjusted R^2 values of 0.73 and 0.69, respectively. In food encapsulation studies, researchers use significant empirical models with moderate explanatory power to establish concentration-dependent encapsulation efficiency. For example, microencapsulation of young barley leaf extract

using maltodextrin, gum arabic, and whey protein isolate yielded an EE model with R^2 and adjusted R^2 of 0.74 and 0.65, respectively, and was statistically significant ($p < 0.05$) (Udo et al., 2026). Moreover, another study used a central composite design to vary the concentrations of chitosan, pectin, and calcium chloride, with moderate predictive power ($R^2 = 0.68$), a significant model ($p < 0.05$), and a non-significant lack-of-fit ($p > 0.05$) (Torpol et al., 2019). Like the models described, the reduced model obtained in this study provides adequate insights for preliminary interpretation of the effects of CS and NaTPP concentrations on GPP encapsulation efficiency within the investigated experimental range. Although its predictive capability is more limited than that of a highly predictive model, the relatively close agreement among the determined R^2 values supports its potential to characterize concentration-dependent relationships rather than serve as a definitive predictive or optimization tool.

The t-ratios indicate the magnitude of each estimated effect relative to its standard error. These statistical results should be interpreted alongside the model's interaction terms and predicted responses to establish whether the combined effects of factors are synergistic or antagonistic (Mercado et al., 2026; Palero et al., 2026). Among the significant model terms and obtained t-ratios, CS concentration emerged as the dominant factor positively associated with the encapsulation efficiency (EE) of the CS-TPP matrices, whereas NaTPP exhibited a nonlinear effect. The positive linear coefficient of CS concentration in the reduced model indicates that increasing CS concentration was associated with higher encapsulation efficiency (EE) in CS-TPP matrices containing GPP within the investigated concentration range. A similar trend was reported during grape extract encapsulation, where increasing CS-to-extract ratios resulted in higher EE, potentially because greater polymer availability accommodates more bioactive material before saturation (Soleymanfallah et al., 2022). In contrast, the negative quadratic coefficient of NaTPP concentration indicates a nonlinear relationship between NaTPP concentration and EE. This suggests that the effect of NaTPP may change across the investigated concentration range, potentially resulting in a maximum EE at an intermediate NaTPP concentration.

The concentration-dependent effect of NaTPP may be explained by its role as an ionic crosslinker. Increasing NaTPP concentration can initially promote interactions between the protonated amino groups of CS and the negatively charged phosphate groups of TPP- polyanions, thereby facilitating matrix formation and potentially improving cargo retention (Kim et al., 2022). However, the relationship between CS and NaTPP concentrations is not necessarily synergistic because their combined effects depend on the balance between polymer availability and crosslinker concentration (Pérez-Pacheco et al., 2025). This means that although increasing NaTPP may initially enhance crosslinking, its effect on EE depends on the formulation conditions and the extent of crosslinking achieved.

The negative coefficient for the quadratic term NaTPP concentration * NaTPP concentration in the reduced model reveals that at excessively high NaTPP concentrations, encapsulation efficiency may decline. This phenomenon was established in previous literature where rapid and extensive ionic crosslinking may promote the formation of a dense matrix near the surface, potentially restricting cargo incorporation or causing the expulsion of entrapped material during matrix formation in CS-TPP systems (Des Bouillons-Gamboa et al., 2024; Nguyen and Le, 2021; Yousefi et al., 2019). NaTPP concentration may also affect particle formation and aggregation, with excessively low CS-to-TPP ratios reportedly increasing turbidity and promoting spontaneous aggregation (Bahreini et al., 2014). Similarly, excessive crosslinker availability may promote aggregation through interactions with existing crosslinked structures (Pérez-Pacheco et al., 2025; Yousefi et al., 2019). Collectively, these findings provide a plausible explanation for the negative quadratic effect of NaTPP observed in the present study, wherein increasing NaTPP concentration may improve EE up to a certain point, beyond which further increases may compromise cargo retention. Accordingly, the quadratic model captures the potential nonlinear relationship between NaTPP concentration and EE within the investigated formulation space.

In addition to the parameters investigated in this study, previous literature has reported that polyphenol release from CS-based encapsulation systems may also vary with parameters such as pH of the surrounding medium, with higher dissolution observed under neutral or near-neutral conditions than under acidic conditions in some systems (Cheng et al., 2023; Pulicharla et al., 2016; Yousefi et al., 2019). These differences were attributed to pH-dependent changes in chitosan protonation, matrix hydration, and polymer relaxation, which may influence polyphenol retention and transport during and after CS-TPP matrix formation (Giraldo et al., 2019). Various studies have reported that the pH of the crosslinking medium may be a relevant parameter to investigate when interpreting encapsulation efficiency (Cheng et al., 2023; Mattu et al., 2013), since some of the polar polyphenols found in crude extracts may be readily soluble in the aqueous phase and may be a cause of limited polyphenol retention (Demircan and Oral, 2023). In this study, the preparation conditions were maintained under neutral conditions, which may have limited the encapsulation performance of the CS-TPP matrices. Examining the encapsulation performance within acceptable pH ranges and the polar and non-polar constituents of the garlic peel polyphenols may lead to a better mechanistic understanding of pH-dependent polymer-core material interactions, leading to desirable encapsulation efficiency.

Characterization of GPP@CS-TPP matrices

The peaks evident along 3000-3600 cm^{-1}, 1550-1650 cm^{-1}, 1090 cm^{-1}, and 900 cm^{-1}, which may be attributed to O–H stretching, N–H (Amide II) bending, C–O stretching, and P–O stretching, respectively (Doğan, 2020; Hssaini et al., 2022; Picar et al., 2025; Varma & Vasudevan, 2020). The broad peak at 3000–3600 cm-1 represents the O-H stretch, which is inherent to CS and also indicates the presence of polyphenols in GPP and GPP @CS-TPP (Basa et al., 2026; Hssaini et al., 2022; Varma and Vasudevan, 2020). The presence of N–H (Amide II) bending on 1550–1650 cm^{-1} bands can also be noted in the spectra containing CS, which is not apparent in GPP since CS contains amino groups (–NH3+) that crosslink with TPP- polyanions, which are not present in the functional groups present in polyphenols (Doğan, 2020; Varma & Vasudevan, 2020). The blue shift between CS and CS-TPP, and between CS and GPP@CS-TPP, may indicate reduced hydrogen bonding and stronger bonding between positively charged amino groups in the CS and the TPP- polyanion. Meanwhile, C–O stretching is observed around 1090 cm-1 (Hssaini et al., 2022). This peak also shows a blue shift, suggesting that positively charged amino groups in CS and the TPP- polyanion crosslink, increasing molecular stability and mechanical strength. Functional groups of the TPP- polyanion were minimally observed, given its low concentration in the matrices. The peak at 900 cm-1 may be attributed to the P=O and P–O bonds in TPP-polyanions, which explains the absence of these peaks in the CS and GPP spectra (Doğan, 2020). The GPP@ CS-TPP and CS-TPP spectra generally show similar behavior, suggesting that encapsulating GPP does not significantly alter the functional groups in standard CS-TPP interactions.

The presence of N–H and P–O bands in the same spectrum indicates ionic complexation between positively charged chitosan amino groups and negatively charged TPP- polyanions. Phosphate functional groups are also present, as shown by the peak around 900 cm^{-1} observed only in spectra of matrices containing TPP, which strongly supports this interpretation. In this regard, FTIR spectroscopy proves the presence of CS-TPP crosslinking, as well as the successful encapsulation of GPP, while the SEM micrograph shown in Figure 5 reveals the hollow structure of the matrix, further supporting the conclusion that the crosslinking using TPP- polyanion occurs quickly on the surface of the matrix, limiting crosslinker diffusion and formation of CS-TPP networks inside the matrices. Higher concentrations of CS and NaTPP cause higher aggregation in the matrices and increased crosslinking density. The amide I and II bands at around 1550–1650 cm-1 show a blue shift in the cross-linked samples compared with CS. More pronounced shifts suggest stronger ionic interactions between the amino and phosphate groups of CS and TPP, respectively, implying greater inter-chain and inter-particle crosslinking and allowing larger aggregates (Hamrayev and Shameli, 2023).

The obtained Feret diameters of CS-TPP and GPP@CS-TPP matrices were significantly larger than what is typically reported in other literature that explores the ionic crosslinking between CS and TPP- polyanions, such as that of Shu and Zhu (2000), which noted a particle size of around 1.2–1.5 mm for matrices formed from 4% CS and 1% NaTPP. Other studies also mainly produce matrices with lower concentrations of CS and NaTPP, yielding smaller nanoparticles. The optimal CS-TPP ratio is 5:1 for nanosized particles, with particle size increasing as the CS-TPP ratio increased (Di Santo et al., 2021). This trend is consistent with previous studies showing significant increases in particle size when CS concentration remained constant and NaTPP concentration decreased (Kim et al., 2022). This agrees with the results of this study, as the GPP-loaded matrices appear to have a higher mean particle size compared to the unloaded CS-TPP matrices. Particle size is also likely affected by polyphenol loading itself, where a substantial increase in particle size was observed as more extract was loaded in the CS-TPP system (Sacco et al., 2021).

The structural heterogeneity of the GPP@CS-TPP network differs clearly from other polymer configurations in the literature. For example, chitosan-coated alginate beads with *Moringa* leaf extract were smooth and spherical but ruptured and broke upon drying because alginate and chitosan amalgamated (Kurtulbaş et al., 2022). This irregular texturing and internal porosity align with trends showing that drug-loaded chitosan nanocomposite formulations exhibit a spherical-like shape with an irregular surface (Chatterjee et al., 2025). However, given that the matrix remains relatively hollow, which implies a porous and flaky structure and a low CS-TPP crosslinking density as shown in the SEM micrograph, it may be deduced that most of the TPP- polyanions rapidly crosslink with the positively charged amino groups in CS at the outer surface, overall affecting the EE of the system. Immediate contact between the positively charged amino groups in CS and the TPP- polyanions forms a rigid surface shell (Sacco et al., 2016, 2021). Previous studies have documented the formation of this rigid surface shell, where morphological observations show a physical barrier that causes chitosan to accumulate at the outer shell, creating a concentration gradient that hinders inward diffusion of TPP ions (Shu and Zhu, 2000). Consequently, this rapid crosslinking often produces an inhomogeneous matrix with a high polymer concentration at the interface and a more liquid core (Sacco et al., 2021). Similarly, crosslinked thiolated starch-coated Fe_3O_4 nanoparticles exhibited a solid, dense, and rough morphology, suggesting a higher and more uniform crosslinking density, similar to the CS-TPP matrices (Saikia et al., 2014). Meanwhile, boric acid-crosslinked beads had irregular pores dispersed throughout their internal structure because of an extremely fast gelation rate and inhomogeneous crosslinking density, which may have caused the same morphological observation in the current matrix (Liao et al., 2018).

Comparison of CS-TPP matrices for encapsulation of bioactive compounds

Previous literature has established successful encapsulation of various bioactive compounds. Empirical studies have validated that altering CS and TPP concentrations can influence the mass, diameter, and water retention capacity of CS-TPP matrices (Giraldo et al., 2019). In addition, the physicochemical properties of the core material may affect the encapsulation performance of a CS-TPP matrix. Previous studies which used CS-TPP to encapsulate hydrophobic core materials, such as resveratrol (99.55%) (Cho et al., 2014), curcumin (95.9%) (Pistone et al., 2023), oregano essential oil (Ma et al., 2022), and astaxanthin (63.9%) (Kim et al., 2022), used compatible solvent-mediated dissolution before extrusion in crosslinking bath, influencing efficient core material entrapment as opposed to direct application in the matrix polymer solution such as that of tetrandine (20.42%) (Iswandana et al., 2017). Hydrophilic core materials such as anthocyanins from purple sweet potato achieved an EE of 31.93% (Laila et al., 2019), which is slightly lower than what was achieved in this study (53.02% ± 10.92%), suggesting that the polarity of the core material due to its dissolution in the crosslinking bath may affect the physical entrapment of these molecules in the matrix. The CS concentration was adjusted to restrict polyphenol mobility by increasing shear resistance through viscosity. At higher concentrations, chitosan chain entanglement improves shear resistance and dissolution (Casella et al., 2026), allowing better retention of the GPP as it is extruded into the crosslinking bath. However, one of the possible trade-offs of this process is the increase in particle size, which is evident since the obtained average particle size of 2.71 mm (2710 μm) for GPP@CS-TPP matrices is significantly higher than the other matrices done in previous studies, in which the largest recorded average particle size is 1,085.95 ± 0.03 μm (Iswandana et al., 2017). This behavior is consistent with empirical studies on how CS and TPP concentrations affect the bead size and weight of the resulting matrices (Giraldo et al., 2019).

In summary, these comparisons show that the encapsulation efficiency of CS-TPP matrices may not depend only on polymer and crosslinker concentrations but also on the physicochemical characteristics of the core material and its compatibility with the encapsulation process. Although several hydrophobic compounds have shown high encapsulation efficiencies, the moderate efficiencies reported for hydrophilic compounds, including anthocyanins, suggest that core-matrix interactions and processing conditions may influence differences in core retention. The study shows that incorporating GPP into CS-TPP matrices is feasible under the investigated formulation conditions. However, this performance should also be interpreted alongside the relatively large particle size, reflecting a trade-off associated with higher chitosan concentrations. Overall, these findings underscore the importance of balancing encapsulation efficiency and particle size when designing CS-TPP matrices for polyphenol delivery. At the same time, further comparative experiments are needed to determine how polarity, viscosity, and crosslinking conditions contribute to encapsulation performance.

CONCLUSIONS

This study successfully encapsulated GPP in water-soluble CS-TPP matrices via ionotropic gelation across varying CS and NaTPP concentrations, achieving a maximum encapsulation efficiency of 53.02% ± 10.92% at 7% CS concentration and 1% NaTPP concentration. FTIR spectroscopy confirmed interactions between the positively charged amino groups of CS and the TPP- polyanion, as well as the successful integration of GPP in the matrices. Particle size analysis showed that the formed matrices were in the macro-particle range (2.71 mm), indicating trade-offs between increasing CS concentration and the resulting particle size distribution. SEM micrographs also revealed successful formation of CS-TPP matrices with low crosslinking density towards the core of the matrix. While CS-TPP is a viable encapsulation system for agricultural waste-derived crude extracts, further investigation of polymer-to-polymer crosslinking interactions, particularly under varying encapsulation pH and crosslinking time, is needed better to understand crude polyphenol extract encapsulation in a CS-TPP matrix. Since only encapsulation efficiency was considered for the study, optimizing other encapsulation metrics, such as particle size and loading capacity, may help address industrial requirements that require certain particle size ranges or material economy. The encapsulation efficiency obtained in the study suggests moderate potential for stabilizing and storing agricultural waste-derived bioactive compounds as crude extracts in CS-TPP matrices. Investigating additional parameters that may influence the encapsulation process, such as encapsulation pH and polymer-to-core material ratios, could provide further insights into improving the encapsulation performance of CS-based matrices. Due to the exploratory nature of the study, the storage stability, release properties, toxicity, and bioavailability of the GPP-encapsulated CS-TPP matrices could potentially provide additional information on their applicability in the food, healthcare, and packaging industries.

FUNDING SOURCE

The authors received no financial support for this research.

ACKNOWLEDGMENTS

The authors would like to acknowledge Ms. Nadine H. Devera for her support in the early conceptualization of this study, and Ms. Ma. Patricia May Cortez of the Department of Science and Technology, Engineering, and Mathematics. The authors would also like to acknowledge the De La Salle University Department of Science, Technology, Engineering, and Mathematics, The Academy; the Department of Chemical Engineering, Gokongwei College of Engineering; and the Department of Chemistry, College of Science, for providing the facilities needed to complete the research work.

AUTHOR CONTRIBUTIONS

L.M.T.U.T., N.J.T.G., B.H.A.D.R., J.J.T.S., C.F.M, and J.R.C.E: Conceptualization; L.M.T.U.T., N.J.T.G., B.H.A.D.R., J.J.T.S., and J.R.C.E: Introduction; L.M.T.U.T., N.J.T.G., B.H.A.D.R., J.J.T.S., and J.R.C.E: Methodology; L.M.T.U.T., N.J.T.G., B.H.A.D.R., J.J.T.S., and J.R.C.E: Data Gathering; L.M.T.U.T., N.J.T.G., B.H.A.D.R., J.J.T.S., and J.R.C.E: Formal Analysis; L.M.T.U.T., N.J.T.G., B.H.A.D.R., J.J.T.S., and J.R.C.E: Investigation; L.M.T.U.T., N.J.T.G., B.H.A.D.R., J.J.T.S., and J.R.C.E: Visualization; C.F.M and J.R.C.E: Writing - Review and Editing. All authors have read and agreed to the publication of this manuscript.

DECLARATIONS

Informed consent statement

None is needed in the study.

Conflicts of interest

The authors declare no conflict of interest.

AI Declaration

Artificial intelligence (AI) tools were used only to assist with language editing, grammar checking, and improvement of clarity during manuscript preparation and revision. The authors reviewed and verified all AI-assisted suggestions and remain fully responsible for the manuscript's accuracy, originality, interpretation, and final content. AI tools were not used to generate, fabricate, or manipulate research data, results, or references.

REFERENCES

Adelpour, T., Mojtabavi, S., Mahmoudabadi-Arani, Z., Bozorgi-Koshalshahi, M., and Faramarzi, M. A. (2025). Green valorization of garlic peel waste using halophilic laccase for efficient biomass delignification and biorefinery applications. Scientific Reports, 15(1), 15885. https://doi.org/10.1038/s41598-025-99715-0

Alara, O. R., Abdurahman, N. H., and Ukaegbu, C. I. (2021). Extraction of phenolic compounds: A review. *Current Research in Food Science, 4*, 200–214. https://doi.org/10.1016/j.crfs.2021.03.011

Althumairy, D. A., Abu-Khudir, R., Alandanoosi, A. I., and Badr, G. M. (2025). Garlic Peel-Derived Phytochemicals Using GC-MS: Antioxidant, Anti-Inflammatory, and Anti-Apoptotic Effects in Ulcerative Colitis Rat Model. *Pharmaceuticals*, 18(7), 969. https://doi.org/10.3390/ph18070969

Assadpour, E., and Jafari, S. M. (2019). Advances in Spray-Drying Encapsulation of Food Bioactive Ingredients: From Microcapsules to Nanocapsules. *Annual Review of Food Science and Technology*, 10, 103–131. https://doi.org/10.1146/annurev-food-032818-121641

Azmat, F., Imran, A., Islam, F., Afzaal, M., Zahoor, T., Akram, R., Aggarwal, S., Rehman, M., Naaz, S., Ashraf, S., Hussain, G., A. R. Suleria, H., Ali, Q., Bibi, M., Batool, F., Gul, F., Amjad, N., and Asif Shah, M. (2023). Valorization of the phytochemical profile, nutritional composition, and therapeutic potentials of garlic peel: A concurrent review. *International Journal of Food Properties*, 26(1), 2642–2655. https://doi.org/10.1080/10942912.2023.2251713

Bahreini, E., Aghaiypour, K., Abbasalipourkabir, R., Mokarram, A. R., Goodarzi, M. T., and Saidijam, M. (2014). Preparation and nanoencapsulation of l-asparaginase II in chitosan-tripolyphosphate nanoparticles and in vitro release study. *Nanoscale Research Letters*, 9(1), 340. https://doi.org/10.1186/1556-276X-9-340

Bamigbade, A. A., Oduntan, K. D., Sulaiman, T. R., Ayeni, I., Olaniyan, J. O., and Akiode, K. O. (2025). Electrochemical Characterization of Non-Enzymatic Glucose Biosensor Based on Silver Nanoparticle (AgNPs) Stabilized with Sodium Tripolyphosphate (NaTPP) Cross-linked Chitosan. *Journal of Chemical Society of Nigeria*, 50(1). https://doi.org/10.46602/jcsn.v50i1.1034

Barbosa-Nuñez, J. A., Espinosa-Andrews, H., Cardona, A. A. V., and Haro-González, J. N. (2025). Polymer-based encapsulation in food products: A comprehensive review of applications and advancements. *Journal of Future Foods*, 5(1), 36–49. https://doi.org/10.1016/j.jfutfo.2024.01.003

Basa, B. A. S. J., Batin, C. D. Z., Chan, I. N. M. D., Gabay, A. R. B., Estrellado, J. R. C., Rallos, R. G. R., Carranza, M. S. S., Lim, M. J. U., Marquez, J. C., and Sta Agueda, J. R. H. (2026). Fabrication, Simulation, and Mechanical Characterization of Curcumin-Loaded PVA/PVP Microneedle Arrays Using Custom 3D-Printed Molds. *Polymers*, 18(15), 1912. https://doi.org/10.3390/polym18151912

Bińkowska, W., Szpicer, A., Stelmasiak, A., Wojtasik-Kalinowska, I., and Półtorak, A. (2024). Microencapsulation of Polyphenols and Their Application in Food Technology. *Applied Sciences*, 14(24), 11954. https://doi.org/10.3390/app142411954

Casella, C., Ballaz, S., Luque, R., and Cornelli, U. (2026). Chitosan with defined intrinsic viscosity enables physicochemical entrapment of microplastics under in vitro gastric conditions. *Journal of Materials Chemistry B*, 14(20), 6311–6322. https://doi.org/10.1039/d6tb00654j

Chatterjee, S., Das, A., Datta, P., Thomas, S., and Ghosal, K. (2025). Medium molecular weight chitosan and magnetite based bead as a nanocomposite for delivery of anticancer drug: Development, evaluation and biocompatibility study. *International Journal of Biological Macromolecules*, 293, 139246. https://doi.org/10.1016/j.ijbiomac.2024.139246

Chaudhary, B. U., Lingayat, S., Banerjee, A. N., and Kale, R. D. (2021). Development of multifunctional food packaging films based on waste Garlic peel extract and Chitosan. International *Journal of Biological Macromolecules*, 192, 479–490. https://doi.org/10.1016/j.ijbiomac.2021.10.031

Cheng, X., Zou, Q., Zhang, H., Zhu, J., Hasan, M., Dong, F., Liu, X., Li, J., Wu, Y., Lv, X., Wang, K., Deng, X., Liu, Z., and Jiang, X. (2023). Effects of a chitosan nanoparticles encapsulation on the properties of litchi polyphenols. *Food Science and Biotechnology*, 32(13), 1861–1871. https://doi.org/10.1007/s10068-023-01303-3

Chhouk, K., Uemori, C., Wahyudiono, Kanda, H., and Goto, M. (2017). Extraction of phenolic compounds and antioxidant activity from garlic husk using carbon dioxide expanded ethanol. *Chemical Engineering and Processing: Process Intensification*, 117, 113–119. https://doi.org/10.1016/j.cep.2017.03.023

Cho, A. R., Chun, Y. G., Kim, B. K., and Park, D. J. (2014). Preparation of Chitosan–TPP Microspheres as Resveratrol Carriers. *Journal of Food Science*, 79(4). https://doi.org/10.1111/1750-3841.12395

Cocom, L. M., Wang, H., Tseng, K., and Chu, Y. (2025). The Antimicrobial and Antioxidant Properties of Raw, Aged, and Fermented Garlic: Influence of Processing Methods. *Food Science & Nutrition*, 13(8), e70743. https://doi.org/10.1002/fsn3.70743

Cruz, P. D. S. (2021). *Analysis of Garlic Supply in the Philippines*, 1990-2019 [University of the Philippines Los Baños]. https://www.ukdr.uplb.edu.ph/etd-undergrad/11636/

De Guzman, S. O. (2023). *Highlights on Garlic Production: Ilocos Region, 2022*. Philippine Statistics Authority. https://rsso01.psa.gov.ph/content/highlights-garlic-production-ilocos-region-2022

Demircan, H., and Oral, R. A. (2023). Parameters affecting calcium-alginate bead characteristics: Viscosity of hydrocolloids and water solubility of core material. *International Journal of Biological Macromolecules*, 236, 124011. https://doi.org/10.1016/j.ijbiomac.2023.124011

Des Bouillons-Gamboa, R. E., Montes De Oca, G., Baudrit, J. R. V., Ríos Duarte, L. C., Lopretti, M., Rentería Urquiza, M., Zúñiga-Umaña, J. M., Barreiro, F., and Vázquez, P. (2024). Synthesis of chitosan nanoparticles (CSNP): Effect of CH-CH-TPP ratio on size and stability of NPs. *Frontiers in Chemistry*, 12, 1469271. https://doi.org/10.3389/fchem.2024.1469271

Detsi, A., Kavetsou, E., Kostopoulou, I., Pitterou, I., Pontillo, A. R. N., Tzani, A., Christodoulou, P., Siliachli, A., and Zoumpoulakis, P. (2020). Nanosystems for the Encapsulation of Natural Products: The Case of Chitosan Biopolymer as a Matrix. *Pharmaceutics*, 12(7), 669. https://doi.org/10.3390/pharmaceutics12070669

Di Santo, M. C., D' Antoni, C. L., Domínguez Rubio, A. P., Alaimo, A., and Pérez, O. E. (2021). Chitosan-tripolyphosphate nanoparticles designed to encapsulate polyphenolic compounds for biomedical and pharmaceutical applications – A review. *Biomedicine & Pharmacotherapy*, 142, 111970. https://doi.org/10.1016/j.biopha.2021.111970

Doğan, M. (2020). Preparation of chitosan nanoparticles and characterization studies. *Cumhuriyet Medical Journal*. https://doi.org/10.7197/cmj.vi.795367

Dos Santos, P. C. M., Da Silva, L. M. R., Magalhaes, F. E. A., Cunha, F. E. T., Ferreira, M. J. G., and De Figueiredo, E. A. T. (2022). Garlic (Allium sativum L.) peel extracts: From industrial by-product to food additive. *Applied Food Research*, 2(2), 100186. https://doi.org/10.1016/j.afres.2022.100186

English, M., Okagu, O. D., Stephens, K., Goertzen, A., and Udenigwe, C. C. (2023). Flavour encapsulation: A comparative analysis of relevant techniques, physiochemical characterisation, stability, and food applications. *Frontiers in Nutrition*, 10, 1019211. https://doi.org/10.3389/fnut.2023.1019211

Estevinho, B. N., and López-Rubio, A. (2024). Recent Advances in Encapsulation for Food Applications. *Foods*, 13(4), 579. https://doi.org/10.3390/foods13040579

Fortunata, S. A., Rahmawati, D., and Andika, D. (2019). Evaluation of Phytochemical Activities of Aqueous and Ethanolic Garlic Peel Extract. *Journal of Functional Food and Nutraceutical*, 1(1), 41–46. https://doi.org/10.33555/jffn.v1i1.20

Giraldo, J. D., Campos-Requena, V. H., and Rivas, B. L. (2019). Chitosan–tripolyphosphate bead: The interactions that govern its formation. *Polymer Bulletin*, 76(8), 3879–3903. https://doi.org/10.1007/s00289-018-2574-9

Hamrayev, H., and Shameli, K. (2023). Synthesis and Characterization of Ionically Cross-Linked Chitosan Nanoparticles. *Journal of Research in Nanoscience and Nanotechnology*, 7(1), 7–13. https://doi.org/10.37934/jrnn.7.1.713

Hernández Zarate, M. S., Abraham Juárez, M. D. R., Cerón García, A., Ozuna López, C., Gutiérrez Chávez, A. J., Segoviano Garfias, J. D. J. N., and Avila Ramos, F. (2018). Flavonoids, phenolic content, and antioxidant activity of propolis from various areas of Guanajuato, Mexico. *Food Science and Technology*, 38(2), 210–215. https://doi.org/10.1590/fst.29916

Hernández-Montesinos, I. Y., Carreón-Delgado, D. F., Ocaranza-Sánchez, E., Ochoa-Velasco, C. E., Suárez-Jacobo, Á., and Ramírez-López, C. (2023). Garlic (*Allium sativum*) peel extracts and their potential as antioxidant and antimicrobial agents for food applications: Influence of pretreatment and extraction solvent. *International Journal of Food Science & Technology*, 58(12), 6794–6805. https://doi.org/10.1111/ijfs.16652

Hssaini, L., Razouk, R., and Bouslihim, Y. (2022). Rapid Prediction of Fig Phenolic Acids and Flavonoids Using Mid-Infrared Spectroscopy Combined With Partial Least Square Regression. *Frontiers in Plant Science*, 13, 782159. https://doi.org/10.3389/fpls.2022.782159

Igathinathane, C., Pordesimo, L. O., Columbus, E. P., Batchelor, W. D., and Methuku, S. R. (2008). Shape identification and particles size distribution from basic shape parameters using ImageJ. *Computers and Electronics in Agriculture*, 63(2), 168–182. https://doi.org/10.1016/j.compag.2008.02.007

Iswandana, R., Putri, K. S. S., Dwiputra, R., Yanuari, T., Sari, S. P., and Djajadisastra, J. (2017). Formulation of Chitosan Tripolyphosphate-Tetranding Beads Using Ionotropic Gelation Method: In Vitro and In Vivo Evaluation. *International Journal of Applied Pharmaceutics*, 9(5), 109. https://doi.org/10.22159/ijap.2017v9i5.20842

Kim, E. S., Baek, Y., Yoo, H.-J., Lee, J.-S., and Lee, H. G. (2022). Chitosan-Tripolyphosphate Nanoparticles Prepared by Ionic Gelation Improve the Antioxidant Activities of Astaxanthin in the In Vitro and In Vivo Model. *Antioxidants*, 11(3), 479. https://doi.org/10.3390/antiox11030479

Kurtulbaş, E., Albarri, R., Torun, M., and Şahin, S. (2022). Encapsulation of Moringa oleifera leaf extract in chitosan-coated alginate microbeads produced by ionic gelation. *Food Bioscience*, 50, 102158. https://doi.org/10.1016/j.fbio.2022.102158

Laila, U., Rochmadi, R., and Pudjiraharti, S. (2019). Microencapsulation of Purple-Fleshed Sweet Potato Anthocyanins with Chitosan-Sodium Tripolyphosphate by Using Emulsification-Crosslinking Technique. *Journal of Mathematical and Fundamental Sciences*, 51(1), 29–46. https://doi.org/10.5614/j.math.fund.sci.2019.51.1.3

Lasalvia, A., Cairone, F., Cesa, S., Maccelli, A., Crestoni, M. E., Menghini, L., Carradori, S., Marinacci, B., Gallorini, M., Elsallabi, O.,Pesce, M., and Patruno, A. (2022). Characterization and Valorization of 'Sulmona Red Garlic' Peels and Small Bulbs. *Antioxidants*, 11(11), 2088. https://doi.org/10.3390/antiox11112088

Lee, S.-Y., Kim, D.-S., and Kyung, K. H. (2014). Factors influencing the stability of garlic thiosulfinates. *Food Science and Biotechnology*, 23(5), 1593–1600. https://doi.org/10.1007/s10068-014-0216-z

Llarena, N. D., Allam, J. A. G., Angelan, E. B., Cahayon, C. M. C., Lumunsad, M. L., Gildo, P. J. A., Sta. Agueda, J. R. H., and Estrellado, J. R. C. (2026). Microwave-Assisted Extraction (MAE) of Propolis from Tetragonula biroi (Philippine Kiwot Bee) Hives. *Engineering Proceedings*, 124(1), 96. https://doi.org/10.3390/engproc2026124096

Lyngdoh, J., and Ray, S. (2022). Valorization of Garlic Peel as a Potential Ingredient for the Development of Value Added Rice Based Snack Product Pukhelein. *Agriculture and Food Sciences Research*, 9(2), 50–58. https://doi.org/10.20448/aesr.v9i2.4110

Ma, Y., Liu, P., Ye, K., He, Y., Chen, S., Yuan, A., Chen, F., and Yang, W. (2022). Preparation, Characterization, In Vitro Release, and Antibacterial Activity of Oregano Essential Oil Chitosan Nanoparticles. *Foods*, 11(23), 3756. https://doi.org/10.3390/foods11233756

Maietti, A., Marchetti, N., Baraldo, N., Fontana, R., and Tedeschi, P. (2025). Black Garlic Powder as an Ingredient to Enhance the Functional and Sensorial Properties of Bread and Its Shelf Life. *Applied Sciences*, 15(9), 5174. https://doi.org/10.3390/app15095174

Mattu, C., Li, R., and Ciardelli, G. (2013). Chitosan nanoparticles as therapeutic protein nanocarriers: The effect of ph on particle formation and encapsulation efficiency. *Polymer Composites*, 34(9), 1538–1545. https://doi.org/10.1002/pc.22415

Mercado, A. K., Batungbakal, R. A., Gomez, V. J., Estrellado, J. R., Bonto, A., Picar, A., and Domingo, C. J. (2026). *Influence of process variables on the green microwave-assisted low-methoxyl pectin extraction from Calamansi peels using citric acid.* Research Square. https://doi.org/10.21203/rs.3.rs-10662945/v1

Naqvi, S. A. Z., Irfan, A., Zahoor, A. F., Zafar, M., Maria, A., Chand, A. J., and Ashfaq, S. (2020). Determination of antimicrobial and antioxidant potential of agro-waste peels. *Anais Da Academia Brasileira de Ciências*, 92(2), e20181103. https://doi.org/10.1590/0001-3765202020181103

Nguyen, G. H., and Le, X. T. (2021). Palmarosa essential oil encapsulated in chitosan nanoparticles by ionotropic gelation: Formulation and characterization. *IOP Conference Series: Earth and Environmental Science*, 947(1), 012002. https://doi.org/10.1088/1755-1315/947/1/012002

Palero, H. C. F., Bobadilla, H. M. I., Ramiso, P. S. B., Madrazo, C. F., and Estrellado, J. R. C. (2026). Green Extraction and Sustainability Assessment of Total Carotenoids from Carrot (Daucus Carota) Peel Waste using Soybean Oil. *Davao Research Journal*, 17(2). https://doi.org/10.59120/drj.v17i2.575

Pant, A., and Negi, J. S. (2018). Novel controlled ionic gelation strategy for chitosan nanoparticles preparation using TPP-β-CD inclusion complex. *European Journal of Pharmaceutical Sciences*, 112, 180–185. https://doi.org/10.1016/j.ejps.2017.11.020

Pérez-Pacheco, Y., Tylkowski, B., and García-Valls, R. (2025). Chitosan Micro/Nanocapsules in Action: Linking Design, Production, and Therapeutic Application. *Molecules*, 30(2), 252. https://doi.org/10.3390/molecules30020252

Picar, A. E., Molina, B. I., Dejuras, J. F., Veran, M. J., and Estrellado, J. R. (2025). Valorization of Cassava Peel and Shrimp Shell Waste for Bioplastic Film Development: Extraction, Characterization, and Response Modeling. *International Journal of Multidisciplinary: Applied Business and Education Research*, 6(6), 3018–3044. https://doi.org/10.11594/ijmaber.06.06.30

Pistone, A., De Gaetano, A., Piperopoulos, E., and Abate, C. (2023). Effect of Sodium Hydroxide and Tripolyphosphate on Curcumin Release from Chitosan-Based Macroparticles. *Materials*, 16(17), 5850. https://doi.org/10.3390/ma16175850

Preciado-Rangel, P., Marín-Gómez, E. R., Ortega-Ortiz, H., Hernández-Montiel, L. G., Núñez-Ramírez, F., Reyes-Pérez, J. J., and Torres-Rodriguez, J. A. (2025). Chitosan Nanoparticles Enhance Yield and Bioactive Compounds in Melon Fruits. Sci, 7(4), 166. https://doi.org/10.3390/sci7040166

Pulicharla, R., Marques, C., Das, R. K., Rouissi, T., and Brar, S. K. (2016). Encapsulation and release studies of strawberry polyphenols in biodegradable chitosan nanoformulation. *International Journal of Biological Macromolecules*, 88, 171–178. https://doi.org/10.1016/j.ijbiomac.2016.03.036

Rathod, N. B., Nirmal, N. P., Abdullah, S., Surasani, V. K. R., Ranveer, R. C., Kumar, S., Chunhavacharatorn, P., Benjakul, S., and Al-Asmari, F. (2023). Extraction of natural bioactive compounds using clean label technologies and their application as muscle food preservatives. *Frontiers in Sustainable Food Systems*, 7, 1207704. https://doi.org/10.3389/fsufs.2023.1207704

Sacco, P., Paoletti, S., Cok, M., Asaro, F., Abrami, M., Grassi, M., and Donati, I. (2016). Insight into the ionotropic gelation of chitosan using tripolyphosphate and pyrophosphate as cross-linkers. *International Journal of Biological Macromolecules*, 92, 476–483. https://doi.org/10.1016/j.ijbiomac.2016.07.056

Sacco, P., Pedroso-Santana, S., Kumar, Y., Joly, N., Martin, P., and Bocchetta, P. (2021). Ionotropic Gelation of Chitosan Flat Structures and Potential Applications. *Molecules*, 26(3), 660. https://doi.org/10.3390/molecules26030660

Saikia, C., Hussain, A., Ramteke, A., Sharma, H. K., and Maji, T. K. (2014). Crosslinked thiolated starch coated Fe3 O4 magnetic nanoparticles: Effect of montmorillonite and crosslinking density on drug delivery properties. *Starch - Stärke*, 66(7–8), 760–771. https://doi.org/10.1002/star.201300277

Shu, X. Z., and Zhu, K. J. (2000). A novel approach to prepare tripolyphosphate/chitosan complex beads for controlled release drug delivery. *International Journal of Pharmaceutics*, 201(1), 51–58. https://doi.org/10.1016/S0378-5173(00)00403-8

Soleymanfallah, S., Khoshkhoo, Z., Hosseini, S. E., and Azizi, M. H. (2022). Preparation, physical properties, and evaluation of antioxidant capacity of aqueous grape extract loaded in chitosan TPP nanoparticles. *Food Science & Nutrition*, 10(10), 3272–3281. https://doi.org/10.1002/fsn3.2891

Spigno, G., Tramelli, L., and De Faveri, D. M. (2007). Effects of extraction time, temperature and solvent on concentration and antioxidant activity of grape marc phenolics. *Journal of Food Engineering*, 81(1), 200–208. https://doi.org/10.1016/j.jfoodeng.2006.10.021

Stoica, R., Somoghi, R., and Ion, R. (2013). Preparation of Chitosan–Tripolyphosphate nanoparticles for the encapsulation of polyphenols extracted from rose hips. *Digest Journal of Nanomaterials and Biostructure*, 8(3). https://storage.imrpress.com/IMR/DJNB/8/3/955_Stoica.pdf

Subroto, E., Cahyana, Y., Tensiska, Mahani, Filianty, F., Lembong, E., Wulandari, E., Kurniati, D., Saputra, R. A., and Faturachman, F. (2021). Bioactive compounds in garlic (Allium sativum L.) as a source of antioxidantsand its potential to improve the immune system: A review. *Food Research*, 5(6), 1–11. https://doi.org/10.26656/fr.2017.5(6).042

Thach, N. A. (2022). Investigation of the effects of extraction temperature and time on bioactive compounds content from garlic (Allium sativum L.) husk. *Frontiers in Sustainable Food Systems*, 6, 1004281. https://doi.org/10.3389/fsufs.2022.1004281

Torpol, K., Sriwattana, S., Sangsuwan, J., Wiriyacharee, P., and Prinyawiwatkul, W. (2019). Optimising chitosan–pectin hydrogel beads containing combined garlic and holy basil essential oils and their application as antimicrobial inhibitor. *International Journal of Food Science and Technology*, 54(6), 2064–2074. https://doi.org/10.1111/ijfs.14107

Udo, T., He, E., Mummaleti, G., Jiao, Y., Chen, J., Singh, R. K., and Kong, F. (2026). Tailoring soy protein isolate–alginate double emulsion composite gel microcapsules for cheese-like texture and probiotic protection in plant-based cheese analogues. *Frontiers in Food Science and Technology*, 6. https://doi.org/10.3389/frfst.2026.1972949

Varma, R., and Vasudevan, S. (2020). Extraction, Characterization, and Antimicrobial Activityof Chitosan from Horse Mussel *Modiolus modiolus*. *ACS Omega*, 5(32), 20224–20230. https://doi.org/10.1021/acsomega.0c01903

Vergel De Dios, T. P., Luares, M. A., Arboleda, W., Calibara, M. D. C., and Estrellado, J. R. C. (2025). Multi-Objective Taguchi Optimization of Electrospinning Parameters for the Development of Poly-(vinyl alcohol)/Waste Wooden Utensil Nanocellulose/Phycocyanin Electrospun Fibers. *International Journal of Multidisciplinary: Applied Business and Education Research*, 6(6), 3045–3069. https://doi.org/10.11594/ijmaber.06.06.31

Yang, F., Xia, S., Tan, C., and Zhang, X. (2013). Preparation and evaluation of chitosan-calcium-gellan gum beads for controlled release of protein. *European Food Research and Technology*, 237(4), 467–479. https://doi.org/10.1007/s00217-013-2021-y

Yousefi, M., Khorshidian, N., Mortazavian, A. M., and Khosravi-Darani, K. (2019). Preparation optimization and characterization of chitosan-tripolyphosphate microcapsules for the encapsulation of herbal galactagogue extract. *International Journal of Biological Macromolecules*, 140, 920–928. https://doi.org/10.1016/j.ijbiomac.2019.08.122

Zhang, H., Wu, S., Tao, Y., Zang, L., and Su, Z. (2010). Preparation and Characterization of Water-Soluble Chitosan Nanoparticles as Protein Delivery System. *Journal of Nanomaterials*, 2010(1), 898910. https://doi.org/10.1155/2010/898910

© Uy Tan et al. (2026). Open Access. This article published by Davao Research Journal (DRJ) is licensed under a Creative Commons Attribution-Noncommercial 4.0 International (CC BY-NC 4.0). You are free to share (copy and redistribute the material in any medium or format) and adapt (remix, transform, and build upon the material). Under the following terms, you must give appropriate credit, provide a link to the license, and indicate if changes were made. You may do so in any reasonable manner, but not in any way that suggests the licensor endorses you or your use. You may not use the material for commercial purposes. To view a copy of this license, visit: https://creativecommons.org/licenses/by-nc/4.0/

Print-ISSN 2244-4432 Online-ISSN 2984-7125